



Supplement of

Regularized inversion of aerosol hygroscopic growth factor probability density function: application to humidity-controlled fast integrated mobility spectrometer measurements

Jiaoshi Zhang et al.

Correspondence to: Jian Wang (jian@wustl.edu)

The copyright of individual parts of the supplement might differ from the article licence.

S1. Mathematical derivation of the integrated response of humidified tandem differential mobility analyzer (HTDMA)

The theoretical response of the i^{th} D_p^* bin of the HTDMA is

$$R_{i,theo} = E \sum_{j=1}^J c_{cond}(g_j) \int_{g_{j-\frac{1}{2}}}^{g_{j+\frac{1}{2}}} dg \int_0^{+\infty} dD_{p1} \Omega_1[V_{DMA}, \tilde{Z}_p(D_{p1})] \Omega_2[V_i, \tilde{Z}_p(gD_{p1})] + \epsilon_i$$

where $E = R_{tot} \left. \frac{Q_{sh,1}}{Q_{a,1}} \frac{dZ_{p1}}{dD_{p1}} \right|_{D_{p1}^*}$. R_{tot} is the total counts of particles detected by the CPC downstream the second DMA with a

- 5 detection efficiency of 1 for particles above 30 nm (i.e., $\eta_{det}(D_{p2}) = 1$). $Q_{a,1}$ and $Q_{sh,1}$ are the sample and sheath flow rates of the first DMA. $\Omega_1(V_{DMA}, \tilde{Z}_{p1})$ is the transfer function of the first DMA operated with the classifying voltage of V_{DMA} , \tilde{Z}_{p1} is the particle mobility (Z_{p1}) normalized by the first DMA centroid mobility corresponding to V_{DMA} . $\Omega_2[V_i, \tilde{Z}_p(gD_{p1})]$ is the transfer function of the second DMA with a scanning voltage V_i , and $\tilde{Z}_p(gD_{p1})$ is the mobility of humidified particles normalized by the centroid mobility of second DMA. $c_{cond,n}(g, D_{p1})$ represents the growth factor probability density function
- 10 (GF-PDF) for particles with respect to growth factor g , and it is assumed that the GF-PDF is the same for all particles classified by the first DMA at a given voltage, i.e., $c_{cond}(g, D_{p1})$ is independent of D_{p1} . ϵ_i is the error in the measured response. Note that equal aerosol flows are assumed for both the first and second DMAs (i.e., $Q_{a,1} = Q_{s,1}$, $Q_{a,2} = Q_{s,2}$).

S2. Dependences of reconstruction residual and smoothness on the number of GF bins for pre-defined GF-PDFs

- 15 inverted using unregularized LSQ and Tikhonov regularization

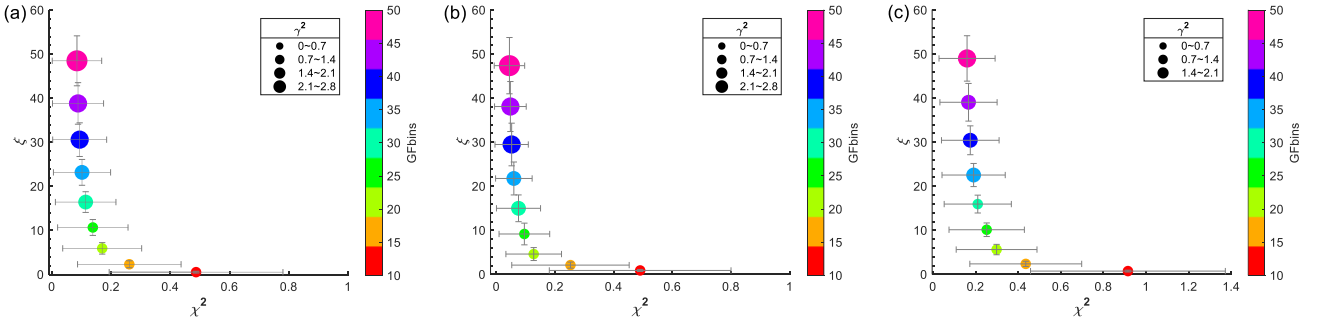


Figure S1. L-curve showing the dependence of reconstruction residual, χ^2 , and the smoothness, ξ , on the number of GF bins of pre-defined GF-PDFs with (a) one mode, (b) two modes, and (c) three modes, respectively. The symbol size represents the error in inverted GF-PDF, γ^2 . Whiskers represent standard deviation. The inversion is conducted using unregularized LSQ method.

20

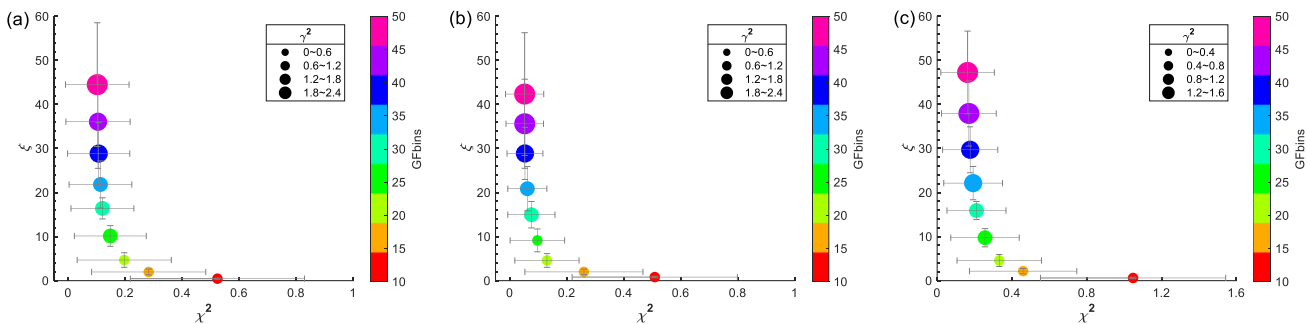


Figure S2. L-curve showing the dependence of reconstruction residual, χ^2 , and the smoothness, ξ , on the number of GF bins of pre-defined GF-PDFs with (a) one mode, (b) two modes, and (c) three modes, respectively. The symbol size represents the error in inverted GF-PDF, γ^2 . Whiskers represent standard deviation. The inversion is conducted using zeroth-order Tikhonov regularization method.

25

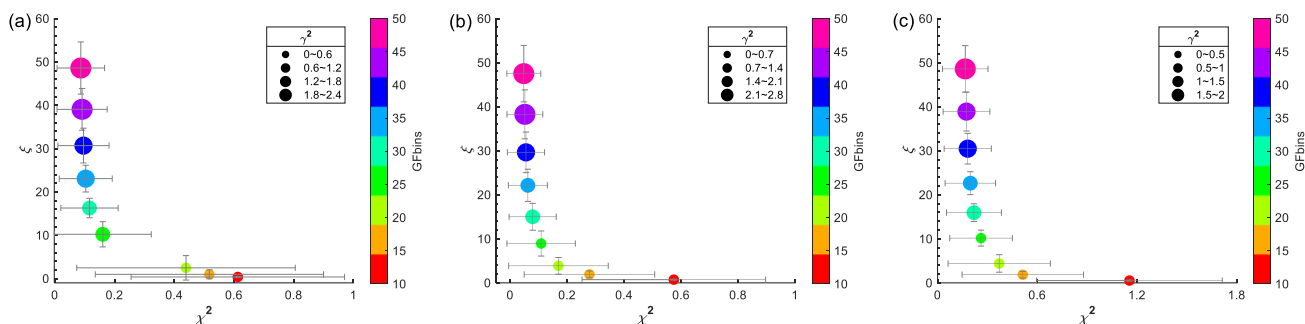


Figure S3. L-curve showing the dependence of reconstruction residual, χ^2 , and the smoothness, ξ , on the number of GF bins of pre-defined GF-PDFs with (a) one mode, (b) two modes, and (c) three modes, respectively. The symbol size represents the error in inverted GF-PDF, γ^2 . Whiskers represent standard deviation. The inversion is conducted using first-order Tikhonov regularization method.

30

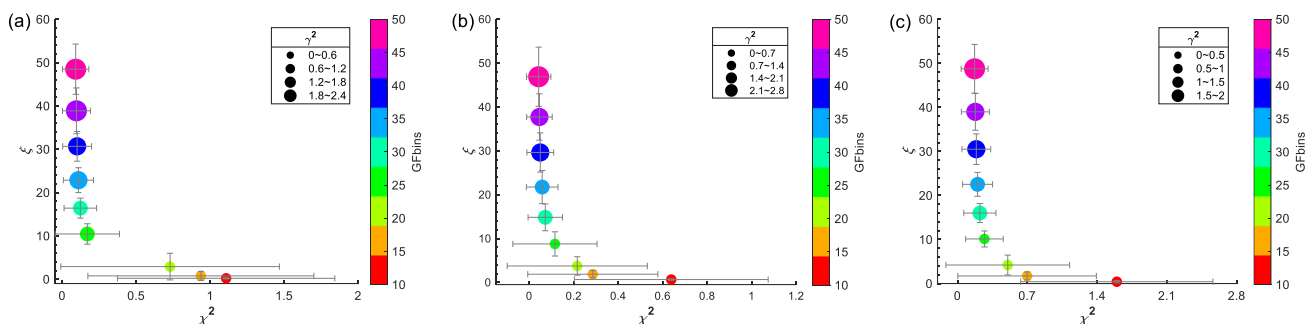
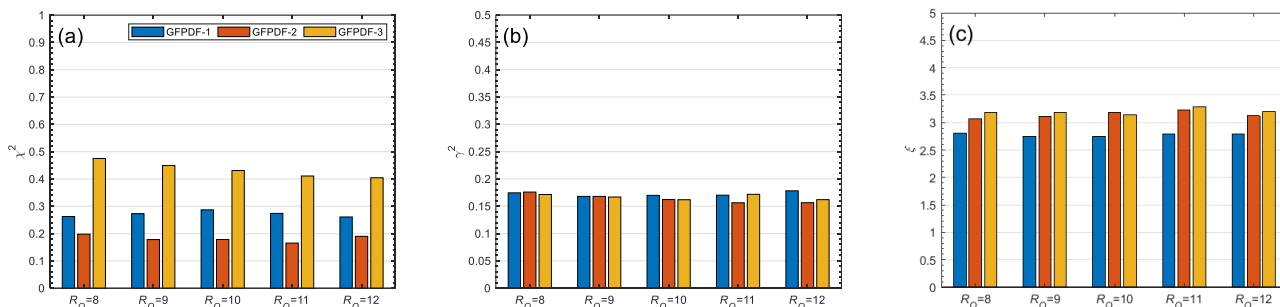


Figure S4. L-curve showing the dependence of reconstruction residual, χ^2 , and the smoothness, ξ , on the number of GF bins of pre-defined GF-PDFs with (a) one mode, (b) two modes, and (c) three modes, respectively. The symbol size represents the error in inverted GF-PDF, γ^2 . Whiskers represent standard deviation. The inversion is conducted using second-order Tikhonov regularization method.

S3. Effect of instrument uncertainties due to calibration nonideality

We also challenged our algorithm with different forward and inverse models to simulate the scenarios when DMA or WFIMS is not perfectly calibrated. The particle sizes measured by DMA and WFIMS are determined by the voltage and sheath flow, which can be calibrated straightforwardly. Therefore, the nonideality in DMA and WFIMS performance likely manifests in the deviation of instrument mobility resolution from the theoretical value. To test the performance of inversion algorithms for such scenarios when the transfer function of DMA or WFIMS is not fully calibrated, we generate the synthetic HFIMS measurements by perturbing DMA or WFIMS mobility resolution (i.e., R_{DMA} or R_{WFIMS}), while maintaining the theoretical R_{DMA} or R_{WFIMS} in the inverse model. The mobility resolution is perturbed by varying the ratio of sheath to aerosol flow rate for DMA or WFIMS ($R_Q = Q_{\text{sh}}/Q_a$) in the derivation of the transfer function. The default flow rate ratio for DMA and WFIMS are 10 and 50, respectively. Figures S5 and S6 show the inversion results when DMA R_Q in the forward model is varied from 8 to 12 while WFIMS R_Q is maintained at the actual value of 50 and when DMA R_Q is maintained at 10 while WFIMS R_Q is varied from 40 to 60. The results are based on inversions of 500 sets of synthetic HFIMS measurements (with the noise of counting statistics included) using Twomey's method. The average residual (χ^2), the GF-PDF error (γ^2), and the smoothness (ξ), all showed very minor variations with DMA or WFIMS R_Q used in the forward model, suggesting negligible impacts on Twomey inversion results due to imperfect calibration of DMA and WFIMS resolution. A possible explanation is that typical GF-PDFs of ambient aerosol particles are relatively broad such that the inverted GF-PDF is insensitive to DMA and WFIMS resolutions. The impact of R_Q on other nonparametric methods was also investigated and found negligible.



50

Figure S5. The reconstruction residual, χ^2 (a), the GF-PDF error, γ^2 (b), and the smoothness, ξ (c) of GF-PDF inverted using Twomey's method as a function of DMA R_Q used to calculate DMA transfer function in the forward model (WFIMS R_Q maintained at the actual value of 50). Actual DMA and WFIMS R_Q values of 10 and 50 are used to derive transfer functions in the inverse model (i.e., calculation of the inversion matrix). The colors correspond to the pre-defined GF-PDFs with one mode (blue), two modes (orange), and three modes (yellow).
 55 The results are averages based on the inversion of 500 sets of synthetic HFIMS data for each of three pre-defined GF-PDFs.

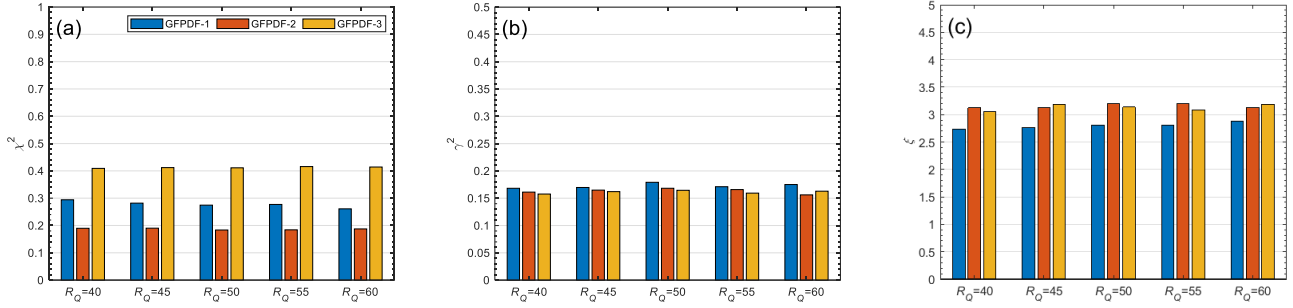


Figure S6. The reconstruction residual, χ^2 (a), the GF-PDF error, γ^2 (b), and the smoothness, ξ (c) of GF-PDF inverted using Twomey's method as a function of WFIMS R_Q used to calculate WFIMS transfer function in the forward model (DMA R_Q maintained at the actual value of 10). Actual DMA and WFIMS R_Q values of 10 and 50 are used to derive transfer functions in the inverse model (i.e., calculation of the inversion matrix). The colors correspond to the pre-defined GF-PDFs with one mode (blue), two modes (orange), and three modes (yellow). The results are averages based on the inversion of 500 sets of synthetic HFIMS data for each of three pre-defined GF-PDFs.

S4. Effect of different level of counting noises

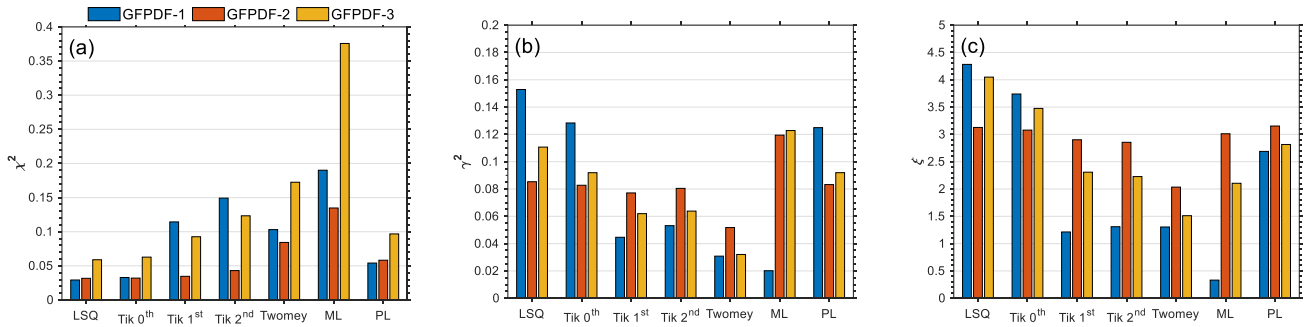
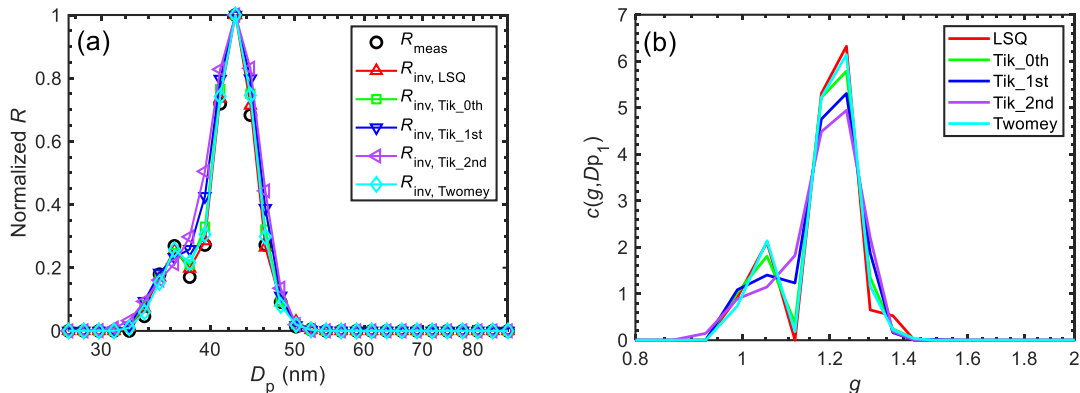


Figure S7. Comparison of reconstruction residual, χ^2 (a), the GF-PDF error, γ^2 (b), and the smoothness, ξ (c) of inverted GF-PDFs using different inversion methods. Colors correspond to the pre-defined GF-PDFs with one mode (blue), two modes (orange), and three modes (yellow). The results are averages based on inversions of 500 sets of synthetic HFIMS data for each of three pre-defined GF-PDFs with total particle counts of 500.

S5. Applications of nonparametric inversion methods to ambient HFIMS measurements

We apply the nonparametric inversion methods to ambient HFIMS measurements, and the results are compared in Fig. S8. The HFIMS responses reconstructed from GF-PDF inverted using unregularized LSQ, Tikhonov, and Twomey's methods generally match the measurement (black circle) well. The GF-PDF at 85% RH for ambient 35 nm particles consist of a smaller less-hygroscopic mode and a larger more-hygroscopic mode. As expected, the HFIMS response reconstructed from LSQ inverted GF-PDF has the minimum deviation from the actual measurement whereas the GF-PDF exhibits oscillations near the tail of the second mode. These oscillations create a small third mode that is absent from the smoother GF-PDFs inverted using

regularized methods (i.e., Tikhonov and Twomey’s methods). GF-PDF inverted using Twomey’s method and zeroth-order Tikhonov clearly distinguish the two growth factor modes. In comparison, the two modes become more overlapped in GF-PDF inverted using first- and second-order Tikhonov regularization, due to additional and possibly excessive regularization.



80

Figure S8. (a) Comparison between the HFIMS measured response (black circle) and the responses (marked lines) reconstructed from GF-PDF derived using different methods for 35 nm ambient aerosol at 85% RH. (b) Inverted GF-PDFs using different methods.

We also examined the statistics of the reconstruction residual and the smoothness of GF-PDF inverted from 3-day HFIMS measurements using the listed nonparametric methods. Among all nonparametric inversion methods, unregularized LSQ leads to the lowest reconstruction residual but the worst smoothness (Fig. S9).

85

As regularizations are introduced in the Tikhonov algorithms, the inverted GF-PDFs become smoother at the expense of increased reconstruction residuals. The Tikhonov regularized solutions strongly depend on the regularization parameter λ . In this study, the value of λ has been derived using three approaches, including (1) the L-curve, (2) the Hanke-Raus rule, and (3) comparison of inverted GF-PDF with the true solution.

90

Note the 3rd approach (i.e., comparison of inverted GF-PDF with the true solution) is not possible for ambient measurements. Inversions of synthetic data show that the L-curve approach generally underestimates the regularization parameter (Fig. 5 in the manuscript), resulting in insufficiently regularized solutions. For the 3-day ambient measurements, when λ is derived using the L-curve approach, the reconstruction residuals for the GF-PDF inverted using Tikhonov algorithms are very close to those of the unregularized LSQ, consistent with underestimated λ values (Fig. S9a and d). In contrast,

95

Tikhonov regularizations with λ value determined using the Hanke-Raus rule tend to over-smooth solutions due to overestimated λ values, resulting in significantly increased errors in reconstructed HFIMS measurements (Fig. S9b and e). The 3-day ambient measurements are also inverted using Tikhonov algorithms with an empirical λ value of 0.03 (Fig. S9c and f), which corresponds to the mean value of optimized λ values (i.e., derived using the 3rd approach) for the synthetic HFIMS data.

100

The inverted GF-PDF shows improved smoothness compared to the solution from the LSQ method, without introducing excessive reconstruction errors. While the empirical λ value appears to work quite well for the 3-day measurements, using this fixed regularization parameter may not be appropriate for other ambient measurements. For Twomey’s method, both the reconstruction residual and the smoothness are between those based on the zeroth- and first-order Tikhonov regularizations with the empirical regularization parameter ($\lambda = 0.03$), suggesting an appropriate trade-off between the GF-PDF smoothness

and the fidelity in reproducing the HFIMS measurements. Note that the statistics of the GF-PDF error cannot be derived as the actual GF-PDF of ambient aerosols are unknown. As a result, it is difficult to draw a definite conclusion regarding which method has the best performance in retrieving the GF-PDF based on the ambient measurements.

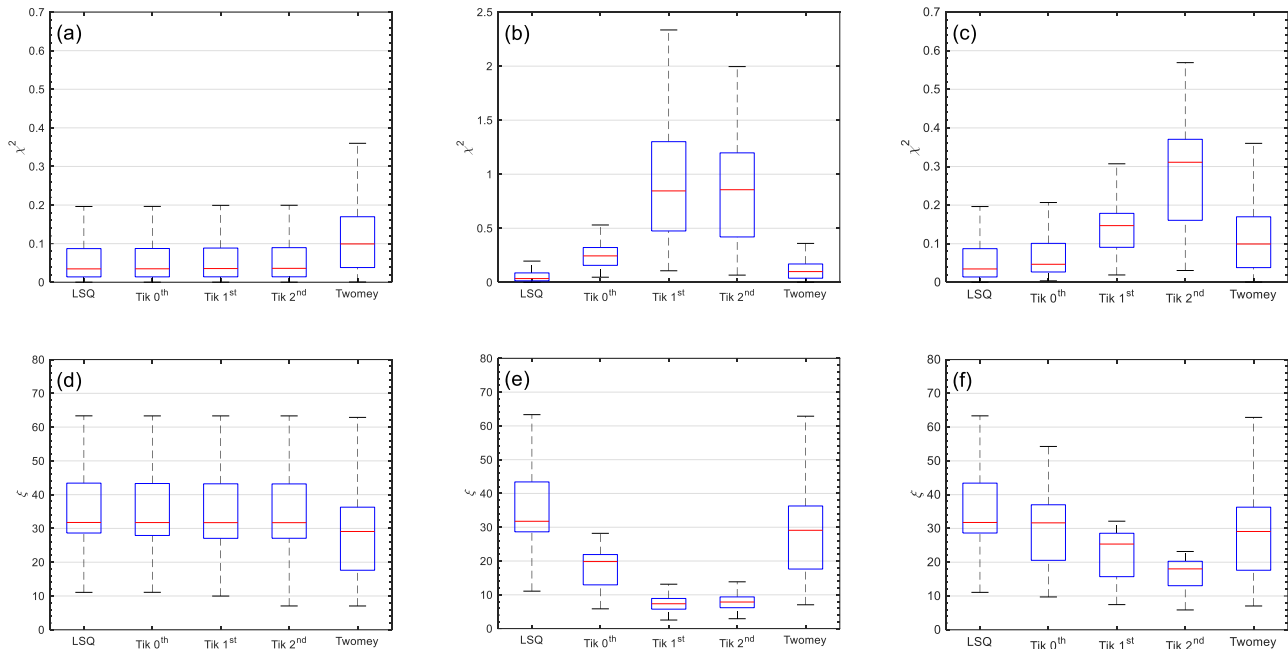


Figure S9. Comparison of reconstruction error, χ^2 (**a, b, c**) and the smoothness, ξ (**d, e, f**) of inverted GF-PDFs using different inversion methods (i.e., LSQ, Tikhonov of zeroth-, first-, and second-order, and Twomey's method), based on three-day HFIMS measurements of ambient aerosols of 35 nm at five different RH levels (20%, 40%, 60%, 75%, and 85%). The Tikhonov regularization parameters are derived using the L-curve approach (**a, d**), the Hanke-Raus rule (**b, e**), and an empirical value of 0.03 (**c, f**), respectively.